Measurement of Drag from Interaction of Jet Exhaust and Airframe

DONALD CHAMBERLAIN*
McDonnell Aircraft Company, St. Louis, Mo.

An investigation was undertaken with a wind-tunnel model specifically designed to measure the drag arising from the interaction of jet exhaust and the surrounding airframe. Three basic nozzle configurations were tested at Mach numbers ranging from 0.60 to 2.48. A one-component axial force balance measured the nozzle afterbody drag. A second one-component balance measured the nozzle thrust minus afterbody drag. This balance was bridged with two air supply lines through a bellows system, which minimized the bridging effects. The model was strut-mounted through the side walls of the transonic and supersonic test sections in the McDonnell Polysonic Wind Tunnel. Cold air, piped into the model through the two strut supports, was used for the jet simulation. Test results were very satisfactory with excellent repeatability and permitted valid configuration comparison.

Nomenclature

D	= afterbody drag
T	= engine thrust
C_D	= afterbody drag coefficient
$C_{(T-D)}$	= thrust-minus-drag coefficient
C_F	= nozzle force coefficient
FB_{fwd}	= force measured by the forward balance
FB_{aft}	= force measured by the aft balance
P	= freestream static pressure
q	= freestream dynamic pressure
P_c	= model internal cavity pressure
P_x	= pressure acting on the afterbody in the seal area
P_{TJ}	= jet total pressure
A_T	= nozzle throat area
A_m	= model cross-sectional area, Fig. 9
A_x	= area on which the seal pressure acts, Fig. 9
Ae_1	= total cross-sectional area of the nozzle, Fig. 9
Ae_2	= total cross-sectional area of the afterbody, Fig. 9
A_{ref}	= maximum model cross-sectional area (reference area)

Introduction

A SUBSTANTIAL portion of total aircraft cruise drag arises from interaction of the jet nozzle exhaust and the flow around the surrounding airframe. Improved nozzle/afterbody configurations significantly improve cruise performance by increasing the difference between engine thrust and afterbody drag.

Previous test setups have provided a measurement of engine thrust-minus-drag coefficient or have provided a measurement of drag coefficient in the presence of a simulated jet nozzle exhaust. The purpose of this paper is to describe the design of a test setup and the test techniques used to measure simultaneously the engine thrust-minus-drag and model afterbody drag. The test equipment and techniques have been successfully used to test the effect of variations in exhaust nozzle configurations. All tests were conducted in the McDonnell Polysonic Wind Tunnel, an intermittent, pressure-to-atmosphere blowdown tunnel with a 4- × 4-ft test section and a Mach number range of 0.5 to 5.8.

Two basic models were used for these tests, both of which were identical in concept and differed only in various construction details. The first model was designed specifically for nozzle-airframe testing, with no attempt made to simulate any particular configuration. The second model, however, was designed to simulate a particular aircraft. Because of the proprietary nature of the second model, all sketches will refer to the nonproprietary configuration of the first model. The test and results were applicable to both models, with the exception that only the second or proprietary configuration was tested above Mach one. The tests were conducted over a range of Mach numbers from 0.6 to 2.48 at Reynolds numbers from 4.5 to 9.5 million/ft. Jet nozzle pressure ratios ranged from 1.6 to 20.0.

A one-component axial force balance (forward balance) measured the difference between the nozzle thrust and the drag force on the nozzle-afterbody combinations. A second one-component axial force balance (aft balance) measured the afterbody drag. Surface pressure distributions were obtained for the afterbody base and nozzle as well as pressure profiles of the fuselage boundary layer. Cold air was used for jet simulation.

Model Design

After having established the desired test objectives of measuring nozzle thrust-minus-afterbody drag and the afterbody drag itself, two basic design problems arose: 1) airframe loads had to be separated from nozzle thrust loads, and 2) high-pressure air at mass flow rates up to 7 lb/sec had to be delivered to the nozzles across the thrust-measuring, one-component balance with a minimum thrust effect. The basic model design concept, shown in Figs. 1 and 2, consisted of a center fuselage support, an afterbody-nozzle combination,

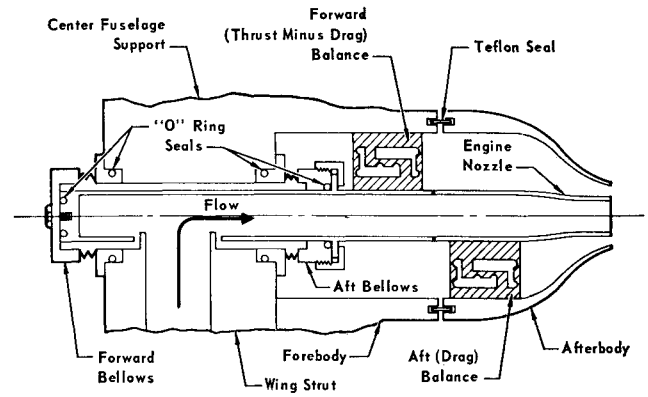

Fig. 1 Model schematic.

Presented as Paper 68-395 at the AIAA 3rd Aerodynamics Testing Conference, San Francisco, Calif., April 8–10, 1968; submitted April 17, 1968; revision received October 9, 1968. The McDonnell Gas Dynamics Laboratories wish to thank B. Corson and J. Runckel of the Langley Research Center, Hampton, Va., for their assistance in the initial model design.

* Laboratory Engineer, Gas Dynamics Laboratory, Engineering Laboratories. Member AIAA.

an engine-nozzle fitting, two combination wing-strut support air-supply ducts, and a forebody.

The engine thrust was measured by mounting the engine nozzle to the center fuselage support with a one-component balance. This is the forward balance shown in Fig. 1. The afterbody drag was determined separately by mounting the afterbody skin on the nozzle assembly with a second one-component balance which is the aft balance shown in Fig. 1. The forward balance then measured the difference between the nozzle thrust and the afterbody drag. All afterbody-nozzle combinations were tested in this manner.

To solve the problem of supplying the high-pressure air across the forward balance, a pair of stainless-steel bellows (Fig. 1) was used in each of the two air supply-lines. The spring constant of the bellows was much lower than that of the forward balance, and therefore nearly all of the engine thrust was reacted through the balance. To reduce further the airflow effects on the forward balance, a liner tube was carried forward from the engine-nozzle block through the aft bellows, center fuselage support, and forward bellows. This tube served as a supply line to the engine-nozzle block and also isolated the bellows from airflow effects, insuring that each bellows would feel the same static pressure. By using a twin bellows arrangement, the loads on the bellows became self-canceling, as an expansion of the forward bellows tended to pull the liner tube forward while an expansion of the aft bellows tended to pull the liner tube aft. The total effect on the forward balance was almost negligible, but the remaining load was accounted for by calibrating the forward balance with air flowing through the model.

The air supply, entering the model through combination wing-support struts, was introduced at right angles to the liner tubes as shown in Fig. 2. Flow straighteners were placed in the struts to insure a straight, uniform flow into the liner tubes. The support-strut air line did not physically touch the liner tube but was pressure-sealed to it by the bellows system. This arrangement allowed the engine nozzle and afterbody assembly to float axially, restricted only by the forward balance and the bellows system. Flow straighteners placed in the liner tubes provided a uniform flow to the nozzles.

The afterbody skins were fiberglass layups or nickel-plated electroforms and were attached to the nozzle assembly through the aft balance. A typical afterbody nozzle assembly is shown in Fig. 3. Two forebody lengths were also made from fiberglass and attached directly to the center fuselage support (Fig. 2). Loads were not measured on these forebodies. Two lengths were required in order to simulate different boundary-layer heights approaching the afterbody. Since the afterbody skin was not attached to the forebody skin, a seal was required between the forward and aft skin to prevent airflow through the model. This was initially accomplished by using a foam-rubber seal between the forebody and afterbody skins. The bridging effect of the seal on the aft balance was accounted for by calibrating the aft balance with the seal installed in the model. Recently, this seal design was changed to one in which a teflon strip lay in a slot cut into both the forebody and afterbody (Fig. 1), which proved to be a more effective seal.

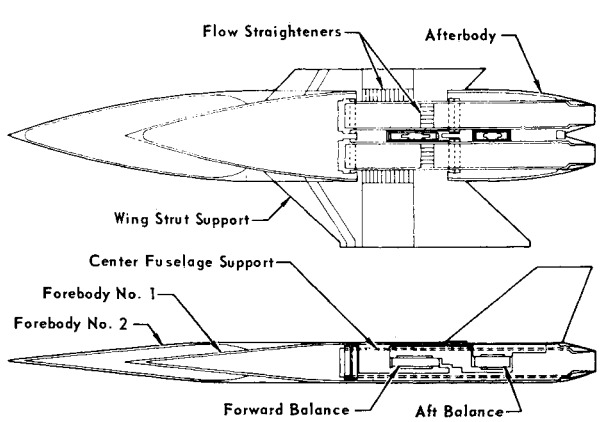

Fig. 2 General assembly.

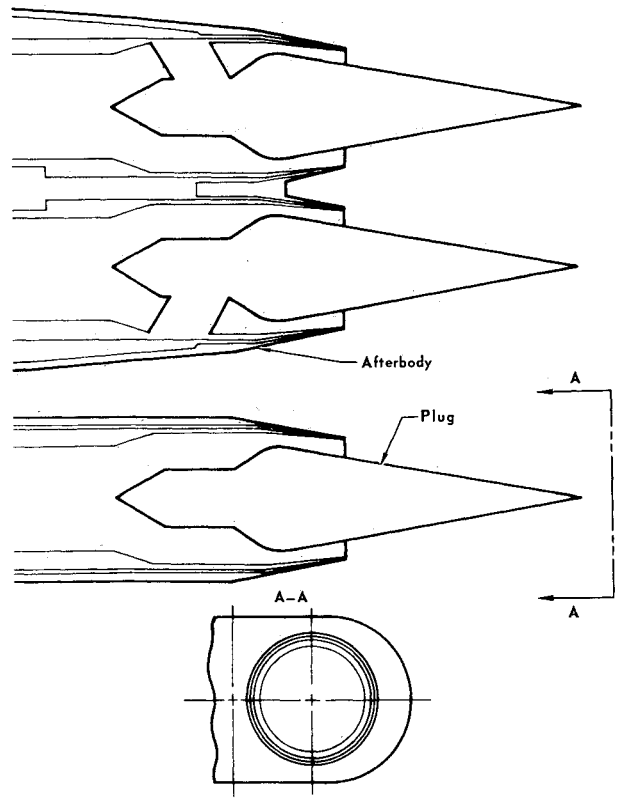

Fig. 3 Plug nozzle-afterbody assembly.

The model was supported in the tunnel's transonic and supersonic test sections with the two combination wing-struts, and was held at a fixed attitude of zero degrees pitch, yaw, and roll. The wing-struts were bolted to the air supply-lines which passed through the test section plenum and up to the walls of the test section. A sufficient amount of the test section walls was removed to allow connection of the air supply-lines to the model support struts. The model was installed in an inverted position to facilitate pressure-tube hook-up, as shown in Figs. 4 and 5.

The air used in the model engine-exhaust simulation was obtained directly from the tunnel compressor that delivers clean, dry air at 600 psia and mass flow rates up to 26 lb/sec. Airflow was controlled with a piston-operated control valve. Operating pressure for this control valve was obtained from an in-house "shop" air supply and controlled with a regulator and a solenoid valve. Jet pressure ratios were set prior to testing by monitoring a duct static pressure and using this pressure to adjust the regulator. A Daniels flowmeter was installed in the airline downstream of the control valve. Downstream of the flowmeter, the 6-in. supply line was split into two 4-in. lines that fed through the test section walls to the model. Controls for the auxiliary air system were located in the tunnel control room.

Each 4-in. air line supplied a separate nozzle. Flow rates were equalized by balancing the static pressure in each nozzle using the two gate valves located in the air supply-lines to the test section. The auxiliary air supply system is shown in Fig. 6.

An important feature of the model design concept was the necessity of keeping the thrust-minus-drag balance very stiff in relation to the bellows. This rigidity was also desired in the aft balance in order to minimize deflections of the afterbody relative to the seal. The balance design was therefore based

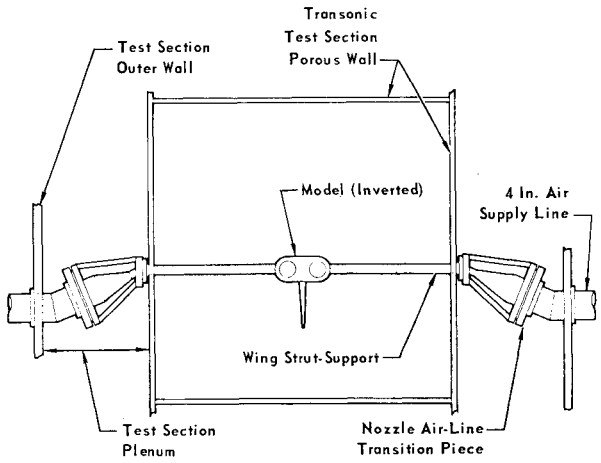

Fig. 4 Tunnel installation; view upstream.

on this need, as well as the additional requirements of simplicity and adaptability to the model. The requirement for stiffness resulted in a low working-stress-level in the flexures (500 to 3000 psi), and, for this reason, semiconductors were used to instrument the balances instead of the more conventional wire strain gages. An additional benefit of the rigid balance was that gages were not required on the normal ele-

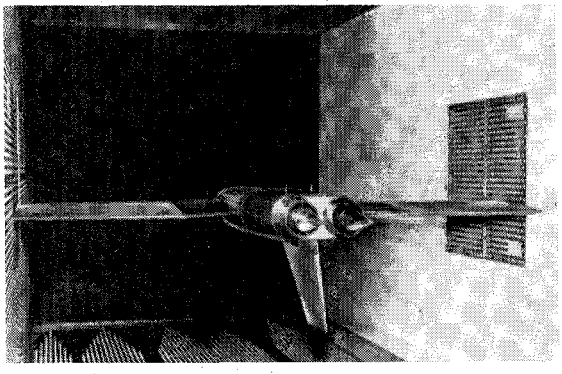

Fig. 5 Tunnel installation.

ments. This was checked by loading the axial balances in a normal direction to determine the interactions, which were found to be negligible.

Model pressures were measured with strain-gage-type pressure transducers that were mounted in holders outside the test section and connected to the pressure pickups by approximately 6 ft of $\frac{1}{16}$-in. tubing routed through the model

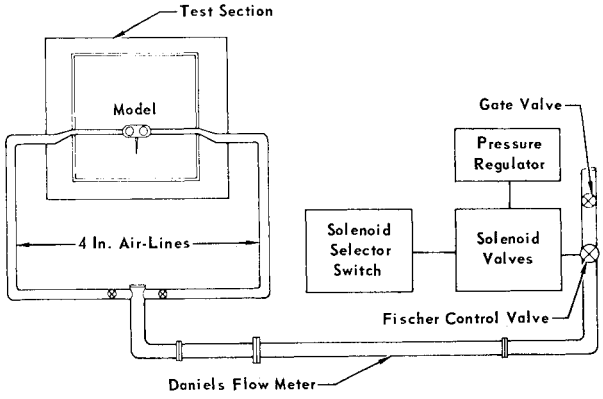

Fig. 6 Nozzle air-supply system.

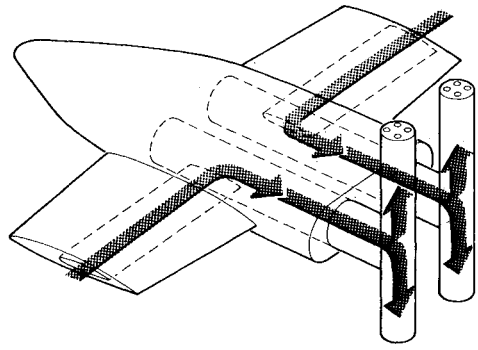

Fig. 7 Zero-thrust nozzles.

struts and into the forebody. All tubes that bridged the thrust-minus-drag balance included a $2\frac{1}{2}$-in. vinyl splice to minimize the bridging of the balance. Recorded pressures included 1) 6 nozzle duct static pressures, 2) 6 model cavity pressures, 3) 7 seal pressures, 4) 4 bellows pressures measured in the plenum between the nozzle ducts and the centerbody, 5) 6 to 21 nozzle surface pressures, depending on the nozzle configuration, and 6) 16 forebody surface boundary-layer pressures. Separate runs were made to measure base pressures on the nozzle afterbodies.

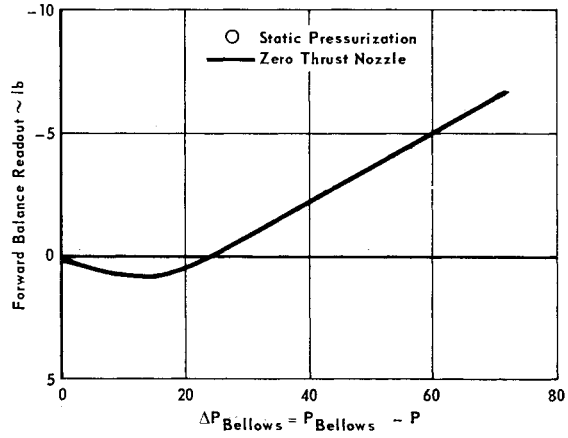

Fig. 8 Forward balance output due to bellows differential pressure.

The Daniels flowmeter was instrumented with two 150-psia transducers, two 5-psi differential transducers, and an iron-constantan thermocouple. Average values of the pressure measurements were used in mass flow rate calculations. Nozzle air temperature was measured with two iron-constantan thermocouples (one in each supply line) just upstream of the model struts. Each afterbody was instrumented to indicate fouling between the jet nozzles and the afterbody.

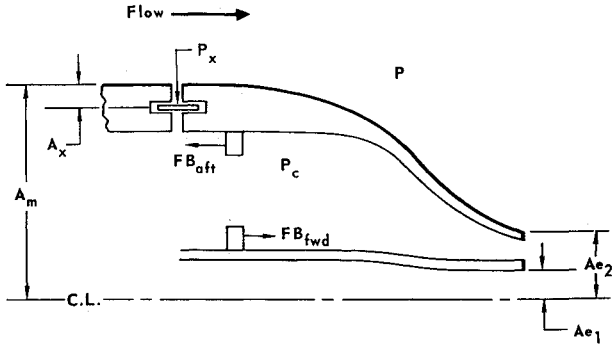

Fig. 9 Reference areas used in data reduction.

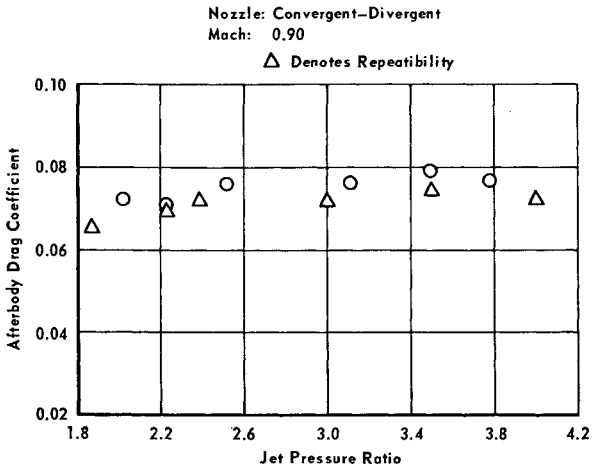

Fig. 10 Afterbody drag coefficient vs jet pressure ratio.

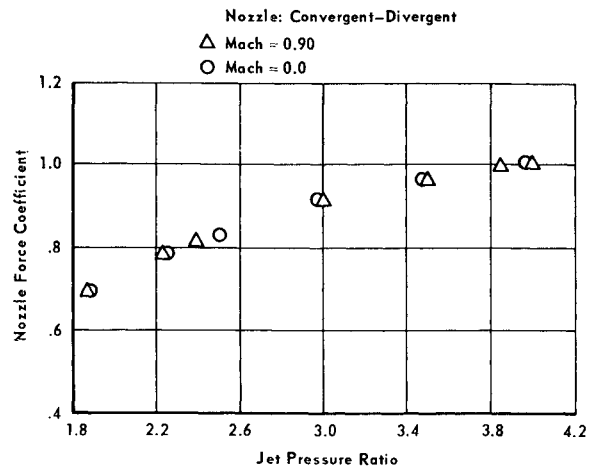

Fig. 12 Nozzle force coefficient vs jet pressure ratio.

As mentioned in the discussion of the model design and fabrication, the forward balance was bridged by the model air-supply, through the bellows system. Though the effect of bridging this balance was small, a calibration program was conducted to measure the extent of bridging and to provide appropriate corrections for the data.

A set of "zero-thrust" nozzles (Fig. 7) was constructed so that all thrust was directed normal to the centerline of the balance. The output of the forward balance was then measured over the range of jet ratios to be used in the wind-tunnel tests. The entire output of the balance with the zero-thrust nozzles installed was due to the bridging effect across the bellows (Fig. 8).

To check further the validity of the bellows bridging, end caps were placed over the nozzles, and the balance was calibrated in a "no-flow" condition at the same duct static pressures as used in the zero-thrust nozzle calibration. It was by no means essential, of course, that agreement be reached between the zero thrust nozzle and the "capped-model" calibration. Experience with the second of the two models mentioned, in fact, indicated a difference between the zero-thrust nozzle and the capped-model results. This emphasized the importance of the zero-thrust nozzle calibration, for without it there could be no real certainty of the validity of the corrections applied to the thrust balance.

All test runs were made at constant Mach numbers with the model at a fixed attitude of zero degrees pitch, yaw, and roll. Prior to each test run, the desired model jet pressure was set using the regulator on the model air-control panel. A final check on all model instrumentation was made, and the tunnel and data system were then brought to a "ready" condition. The jet air was turned on, and after flow stabilization the tunnel was started. Eight scans of data were recorded approximately 1 sec apart, and the model air and the tunnel were then shut down. This procedure was repeated for all nozzle-pressure ratios. The short duration of the run minimized the temperature effects on the afterbody and seal.

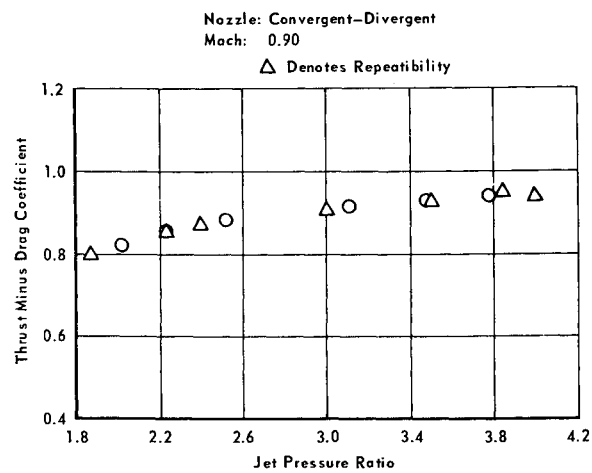

Fig. 11 Thrust-minus-drag coefficient vs jet pressure ratio.

Data Reduction

The afterbody drag coefficient (C_D) was determined from the aft balance load, corrected for model cavity and seal pressure, and nondimensionalized using the maximum model cross-sectional area and freestream dynamic pressure,

$$D = FB_{\text{aft}} - (P_c - P)(A_m - A_x - Ae_1) - (P_x - P)A_x$$
$$C_D = D/A_{\text{ref}}\, q$$

The engine thrust-minus-drag coefficient ($C_{(T-D)}$) was determined from the forward balance reading, corrected for model cavity and seal pressure and nondimensionalized in the same manner as the afterbody drag coefficient

$$(T - D) = FB_{\text{fwd}} + (P_C - P)(A_m - A_x - Ae_2) + (P_x - P)A_x$$
$$C_{(T-D)} = (T - D)/A_{\text{ref}}\, q$$

The reference areas used in these equations are shown in Fig. 9.

Representative values of the afterbody drag coefficient and the engine thrust-minus-drag coefficient are presented in Figs. 10 and 11. These plots show that the data were highly repeatable and that valid comparisons were therefore possible among the various nozzle configurations tested. The nozzle surface and base pressure data were presented in tabulated, dimensionless form as ratios to freestream static pressure. Boundary-layer pressure data were tabulated as ratios to freestream total pressure.

A correlation of static and wind-on nozzle thrust is shown in Fig. 12. These results tend to validate the balance measurements:

C_F = nozzle force coefficient
$C_F = T/P_{TJ} \cdot A_T$
$T = (T - D) + D$
P_{TJ} = calculated jet total pressure
A_T = throat area

Summary

A wind-tunnel model was designed and fabricated for the express purpose of providing test data on the drag level of various nozzle and afterbody configurations. This model

incorporated unique methods to separate nozzle and airframe loads and to bridge the thrust-measuring balance with a high-pressure air-supply system.

Special test procedures involved 1) measuring the amount of bridging of the thrust balance not removed by the bellows system and making the necessary corrections to the data, 2) measuring the extent to which the afterbody-forebody seal bridged both balances, and again making the necessary corrections to the data, and 3) using a short-duration run to minimize temperature effects on the afterbody and seal. Test results were very satisfactory with excellent repeatability, and valid configuration comparisons could be made.

MARCH-APRIL 1969 J. AIRCRAFT VOL. 6, NO. 2

AH-56A Onboard Fueling Capability

F. J. STOCKEMER*
Lockheed-California Company, Burbank, Calif.

The ability to operate from unimproved bases with minimum support equipment was a principal design objective for the Army AH-56A Cheyenne armed compound helicopter being built by Lockheed-California Company. An important element of this concept is the use of the aircraft's boost pump to fuel the ship from drums or other containers through the pressure fueling system. Pump electrical power is furnished by the aircraft's auxiliary power unit. The only ground equipment required is a suitable hose with disconnect fitting to match the ship and storage container. Tests to develop this capability were conducted on a full-scale fuel-system simulator as part of a complete fuel-system test program. With the resulting system, priming time through 38 ft of 1½-in. hose averaged 45 sec; steady-state fueling rate was approximately 50 gal/min. Fueling from large rather than small containers is more efficient because of fewer priming operations.

Discussion

ONE of the most advanced combat aircraft to be developed in recent times is the Lockheed AH-56A Cheyenne being built for the U.S. Army. Its mission is to provide protection for troop-carrying helicopters and to furnish direct-fire support in combat zones. With a design speed of over 250 mph, it is considerably faster than armed helicopters now in Vietnam and carried much more fire power. Figure 1 is a photograph of the AH-56A in flight.

The aircraft is 55 ft long, has a main rotor-blade diameter of 50 ft, and a stub wing with a 27-ft span. It is powered by a General Electric T-64-16 gas turbine engine connected to a main transmission that distributes engine power to the main rotor, the antitorque rotor on the left side of the aircraft, and the thruster propeller at the tail. The engine has a military rating for 30 min of 3400 hp to 76°F, and a cruise rating of 3230 hp. This arrangement provides a standard day hover ceiling, out of ground effect, of 10,600 ft. Maximum rate of climb is over 3400 ft/min. Maximum range with 10% fuel reserve, at design gross weight, is 760 naut miles (874 statute miles), while maximum endurance for the same reserve and gross weight condition is 5.4 hr. By employing short takeoff and landing runs at optimum altitude, with 10% fuel reserve, ferry missions can be flown to a maximum range of 2510 naut miles (2886 statute miles).

Two men constitute the crew, a pilot in the aft seat and a copilot/gunner in the forward seat. Dual controls enable either man to fly the aircraft.

With its outstanding feature of inherent stability, the Lockheed rigid rotor system gives this compound helicopter the high degree of stability and performance that it requires as a modern aerial weapons platform.

Since the Cheyenne is intended to escort other helicopters and to operate in combat zones, one of the principal design criteria was that it be able to operate from small, virtually unimproved sites with a minimum of ground-support equipment. In conformity with this concept, the ship's fuel boost pump for the engine feed system can be used also to suck fuel from drums or other storage containers such as flexible bags, and introduce it into the aircraft's fuel tanks. The only piece of ground-support equipment required is a suitable hose with a disconnect fitting to match the ship's fitting.

To assist in visualizing how this onboard fueling capability is accomplished, Fig. 2 is a schematic diagram of the internal fuel system. Fuel storage consists of three flexible fuel cells with gravity interconnects, having a combined capacity of approximately 440 U.S. gal. The main cell is located in the fuselage aft of the wing box beam, whereas two smaller cells are located in the protruding sponsons forward of the wing, one of which is visible in Fig. 1. In level flight, the bottoms of the sponson cells are above the bottom of the main cell, whereas the tops of the sponson cells are below the top of the main cell. At the aft end of each gravity interconnect is a free-swinging check valve to inhibit flow from the main cell to the sponson cell, and also a standpipe to permit the sponson cells to be fueled by gravity flow from the main cell. A partial bulkhead toward the forward end of the main cell forms a surge box sump for the boost-pump inlet tube. Check valves permit gravity flow from the aft portion of the main cell into the surge box and an ejector operating from boost-pump pressure scavenges fuel from the aft portion of the main cell into the surge box to assure that the boost-pump suction inlet remains immersed in fuel until the internal fuel supply is depleted.

Fuel can be introduced into the internal fuel system by manual fueling through a standard filler opening, through a standard 2½-in. pressure fueling adapter, or from ground storage, using the suction generated by the ship's boost pump.

Presented as Paper 68-560 at the AIAA 4th Propulsion Joint Specialist Conference, Cleveland, Ohio, June 10–14, 1968; submitted June 10, 1968.

* Group Research and Development Engineer, Power Plant Laboratory. Member AIAA.